

# Fracture of Aluminium Alloy 2024 under Triaxial Loading

M. Mostafavi<sup>1</sup>, D.J. Smith<sup>2</sup>, M.J. Pavier<sup>2</sup>

<sup>1</sup>Materials Performance Centre, University of Manchester, The Mill, Manchester, UK  
Email: [M.Mostafavi@manchester.ac.uk](mailto:M.Mostafavi@manchester.ac.uk)

<sup>2</sup>University of Bristol, Queen's Building, University Walk, Bristol, UK

Email: [David.Smith@bristol.ac.uk](mailto:David.Smith@bristol.ac.uk)

Email: [Martyn.Pavier@bristol.ac.uk](mailto:Martyn.Pavier@bristol.ac.uk)

**ABSTRACT** Previous biaxial tests have shown that the fracture toughness measured from standard tests is not the minimum critical  $J$ -integral. This gives rise to the questions: what is the minimum critical  $J$ -integral and how can it be obtained? To answer these questions a triaxial test machine capable of applying loads in three perpendicular directions was designed and built. Conducting triaxial test helps to investigate further the effects of stress state in the fracture of metallic materials, particularly when the plasticity is highly constrained. Although low constraint conditions can be easily achieved by changing the geometry of the test coupons, high constraint (high triaxiality) conditions are difficult to achieve. The primary purpose of this paper is to report the experimental findings of the triaxial tests performed on specimens fabricated from Aluminium Alloy 2024. It was found that indeed high triaxial loading decreases the critical  $J$ -integral below the standard value.

## INTRODUCTION

It is well known that plastic constraint influences the critical  $J$ -integral (energy release rate upon fracture) of metallic materials [1, 2]. The lower the constraint, the more plastic deformation occurs prior to fracture, which in turn causes fracture to occur at a higher load. The standard procedures, therefore, are designed to provide the highest constraint conditions which ensures the specimens to fracture at the lowest load (e.g. [3]). Such procedures are believed to give the most conservative value for the fracture toughness. However, it has been shown that there are conditions where the constraint is even higher than the prescribed conditions recommended by the standards. One of these conditions is multiaxial fracture [4].

The authors have shown through biaxial tests [5] that the critical  $J$ -integral can become lower than those of the standard SEN(B) or C(T) tests if loads in the in-plane or out-of-plane directions are applied (Figure 1). This gives rise to the question: what is the combined effect of applying loads in in-plane and out-of-plane directions simultaneously. The main purpose of this paper is to report the findings of an experimental investigation for specimens made of aluminium 2024 alloy in triaxial tests. Loads in two axes (in-plane and out-of-plane) increase or decrease the constraint level of the specimen and load in the third axis causes the specimen to fracture.

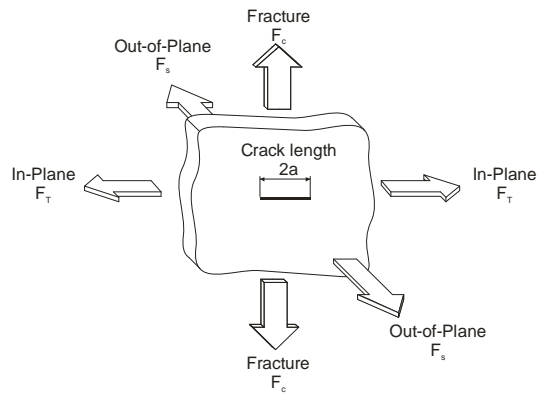


Figure 1- In-plane, out-of-plane and fracture directions in a cracked body

## EXPERIMENTS

Adding a third axis to a biaxial test machine provides the means to apply loads in three perpendicular directions. To this end, a frame was added to the biaxial machine (Figure 2) and a hydraulic actuator was mounted on this frame. Because of the height limitation it was not possible to use another actuator on the bottom of the biaxial rig bed-plate. Therefore a self-contained test jig was designed to attach to the single actuator in the third direction (Figure 3a). As seen in the figure, because the loading area was attached to the body of the actuator, no load was transferred to the frame from the test area.

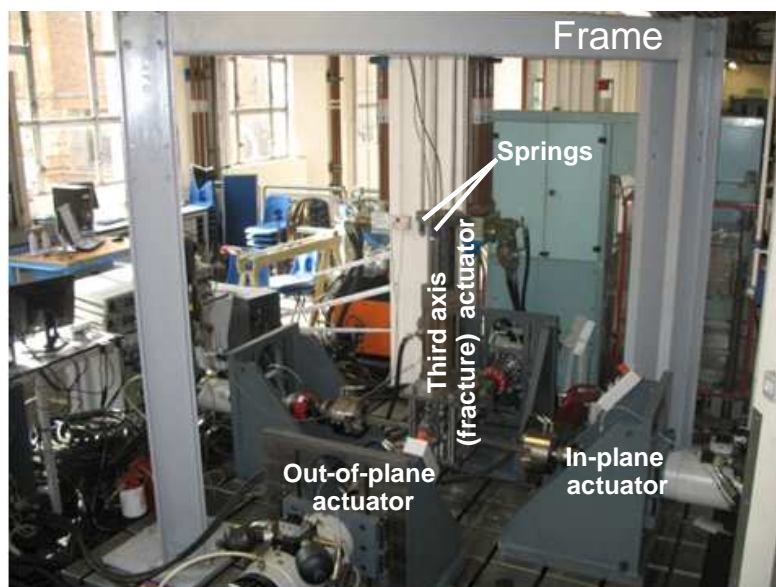
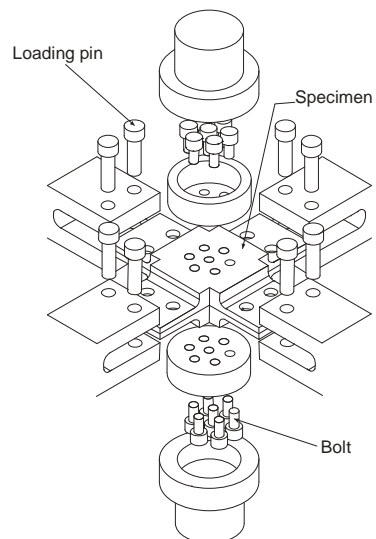


Figure 2- Overview of the triaxial test machine

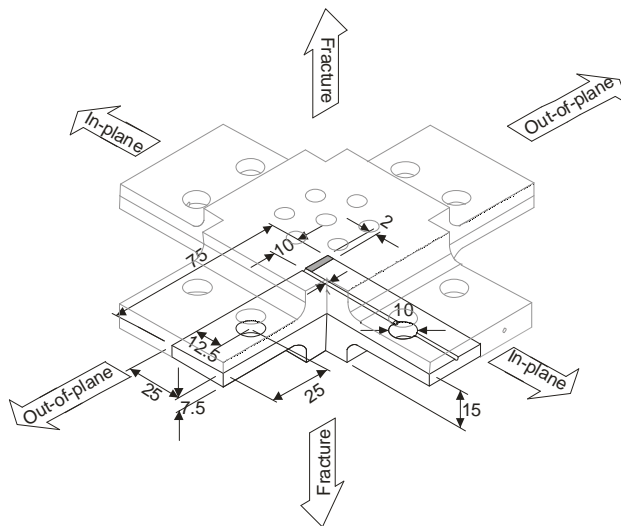
The connection between the actuator and the fixed frame was through four light springs, which made the system self-aligning. Considerable attention was paid to ensure that the 5 actuators were level and aligned. The actuators located horizontally (original biaxial machine) were used to apply loads in the in-plane and out-of-plane directions. The extra actuator in the third direction was used to fracture the specimen. This actuator had a maximum load capacity of 65kN and was controlled by an Instron hydro-controller. The capacity of the horizontal actuators was 100kN and Zwick/Amsler hydro-controllers were used.



(a)



(b)



(c)

**Figure 3- Overview of the triaxial test configuration (a) self-contained third axis (b) schematic view of the test area (c) detail of crack**

The specimens were machined from aluminium alloy 2024, which was manufactured in rolled plate form. The maximum thickness of the plates was 35mm. This plate thickness was not sufficient to satisfy conventional thickness requirements in a fracture mechanics test. To overcome this, the triaxial specimen (Figure 3c) was designed with the extra parts shown in Figure 3b. Seven M6 bolts were used at each side to attach the extra parts to a 30mm thick specimen to form a 150mm long specimen in the fracture direction suitable to be used in the loading jig. A wire electrical discharge machine was used to introduce cracks in the specimens using 0.1mm (diameter) wire. The specimens were cut in the XY plane symmetrically and only a 4×20mm rectangular section was left uncut connecting the two halves of the specimen. A quarter of the uncut area is shaded gray in Figure 3c. The short edge of the ligament was cut in the form of 1mm circular section to make sure that the crack propagation started from the long edge.

Because two separate sets of controllers were used, one for the horizontal (biaxial) loading and one for the extra actuator in the third direction, it was not possible to apply the in-plane, out-of-plane and fracture loads simultaneously in displacement control. Therefore, the in-plane and out-of-plane loadings were applied as a preload at a rate of 6kN/min, and then kept constant throughout the rest of the test. The fracture load was then applied. To attain quasi-static conditions, the displacement in the fracture direction was applied with the rate of 0.1mm/min. FE analyses were carried out before the test to ensure no plasticity occurred during the preloading stage.

Different in-plane and out-of-plane loads were considered for 10 triaxial specimens. The preloading levels along with the corresponding fracture loads are given in Table 1.

Table 1- Fracture loads of specimens with different in-plane and out-of-plane loadings

<b>Specimen</b>	<b>In-plane preload <math>F_T</math> (kN)</b>	<b>Out-of -plane preload <math>F_S</math> (kN)</b>	<b>Fracture load <math>F_c</math> (kN)</b>
<b>T01</b>	2	2	55.72
<b>T02</b>	90	90	58.89
<b>T03</b>	60	60	55.60
<b>T04</b>	90	90	56.46
<b>T05</b>	2	2	54.53
<b>T06</b>	2	90	50.04
<b>T07</b>	2	90	49.47
<b>T08</b>	90	90	57.73
<b>T09</b>	2	90	49.43
<b>T10</b>	30	90	52.47

## FINITE ELEMENT ANALYSIS

Finite element analysis was performed to calculate the critical  $J$ -integral of the specimens to enable the effect of constraint to be examined. A total number of 13000 twenty-node brick elements were used to model one eighth of the triaxial specimen. Figure 4 shows both the overview and near crack tip details of the finite element model. It was postulated that friction between the loading pins and the specimen might apply a noticeable closing load on the two halves of the specimen. Therefore, half of each loading pin was also simulated in the FE model with contact defined between the specimen and the pins. Because the loading pins were made of steel, much stiffer than the aluminium specimen, it was deemed appropriate to use rigid elements for modelling them. Suitable boundary conditions were applied to the model. Similar to the experiments, which were performed in two stages, the simulation was performed in two steps for each loading condition. In the first step, loads were applied in the two transverse directions. The  $J$ -integral was calculated at this stage by ABAQUS [6] using the contour integral method [7]. In all cases the  $J$ -integral was zero since no opening load was acting on the crack. The second step applied the fracture load in the third direction.

A number of different parameters were extracted from the FE model. The maximum critical  $J$ -integral along the crack front at the fracture load is reported in Table 2. Stress triaxiality factor at  $r_c = 500\mu\text{m}$  was extracted from the FE analysis and also reported in Table 2. The variation of the critical  $J$ -integral as a function of the stress triaxiality factor is shown in Figure 5.

Table 2- Details of constraint measures in triaxial specimens for different in-plane and out-of-plane loadings

Specimen	Critical $J$ -integral $J_c$ (MPa.mm)	Stress triaxiality factor $T_f$ at $r_c = 0.5\text{mm}$
T01	36.91	2.19
T02	20.18	2.52
T03	22.23	2.47
T04	20.21	2.54
T05	33.76	2.24
T06	23.07	2.36
T07	21.86	2.36
T08	20.66	2.53
T09	24.28	2.36
T10	20.70	2.43

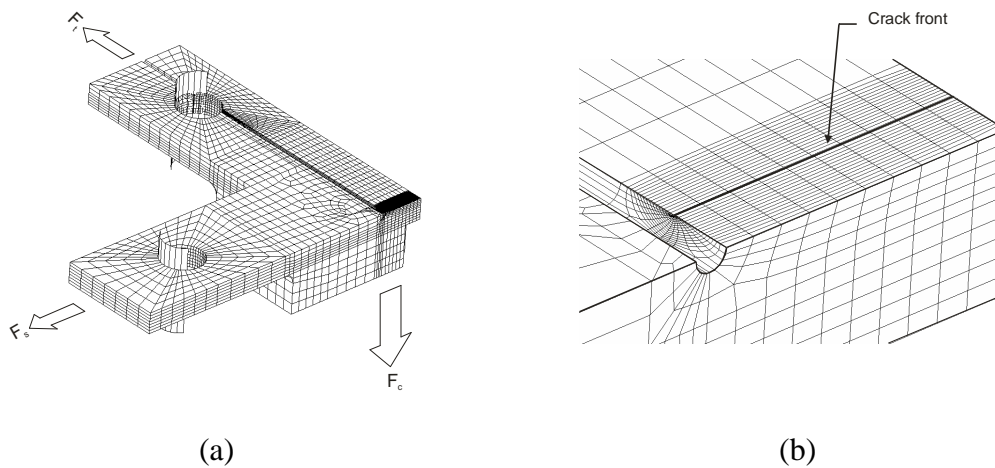


Figure 4- Finite element model of the triaxial specimen (a) general overview (b) details of the cracked area

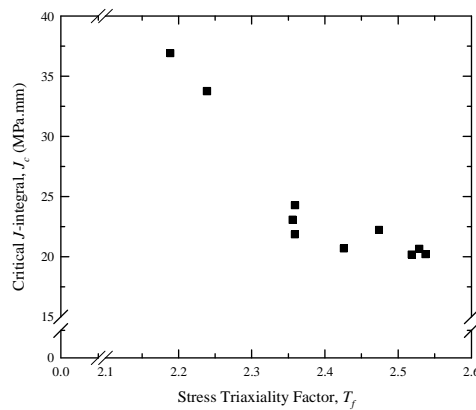


Figure 5- Critical  $J$ -integral variation versus the stress triaxiality factor at the characteristic distance of the triaxial test specimens.

## DISCUSSION

Since both in-plane and out-of-plane loadings were applied to these specimens causing a variation in both in-plane and out-of-plane constraint levels, conventional constraint quantifying parameters such as T-stress or Q do not seem appropriate as they are confined to measure the level of in-plane constraint. The stress triaxiality factor on the other hand can be used to consider both in-plane and out-of-plane loadings. Table 2 shows that when in-plane and out-of-plane loadings were applied to the specimens, the triaxiality factor increased. Figure 5 shows the critical  $J$ -integral values versus the stress triaxiality factor at  $r_c = 500\mu\text{m}$  in the triaxial specimens. The figure demonstrates that the critical  $J$ -integral decreased as the triaxiality factor increased.

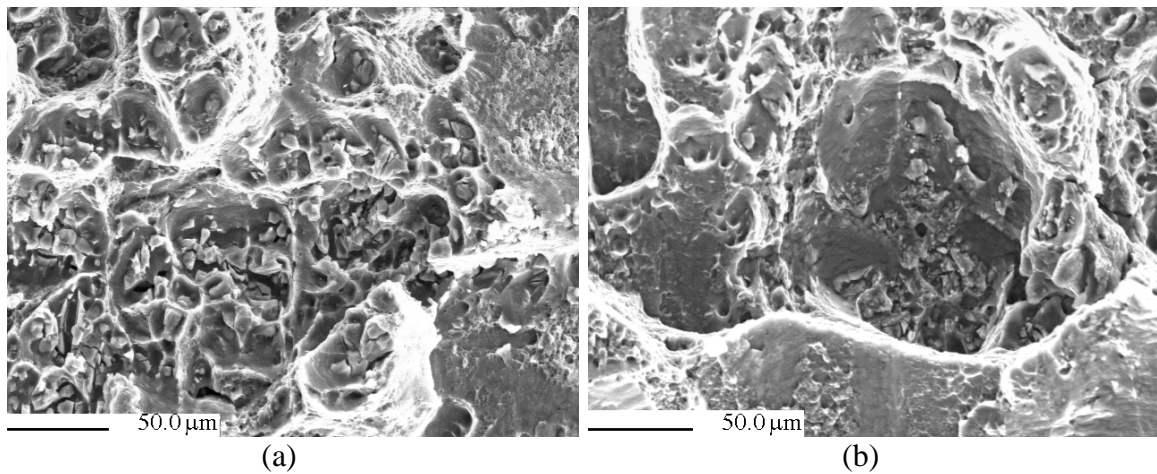


Figure 6- SEM images of the fracture surface (a) No transverse loading (b) 90kN transverse load in in-plane and out-of-plane directions

Finite element modelling of the triaxial test showed that there was a significant effect of friction induced between the loading pins and the specimen. This was because of the configuration of the test where the loading pins not only applied loads in the in-plane or out-of-plane directions, they also gripped the specimen and prevented it from opening freely. It was evident that with more transverse load, greater friction load was induced to prevent opening. Results in Tables 1 and 2 show that although the fracture loads of specimens T02, T04 and T08, with 90kN applied in both in-plane and out-of-plane directions, were higher than specimens T01 and T05, with only 2kN transverse loads, they had in fact exhibited a lower critical  $J$ -integral. Thus, a portion of the load in the third axis was used to overcome the friction.

The triaxial specimen was designed in a way that, even without applying any transverse loading, it had a high constraint level. Plane strain conditions prevail in the middle of the crack front (high out-of-plane constraint) and  $T$ -stress was positive (high in-plane constraint). It is therefore expected that the critical  $J$ -integral obtained from the triaxial test without transverse load would be close to the fracture toughness obtained from a standard test. Figure 5 shows that the critical  $J$ -integral in the triaxial specimen without any transverse load was about 35MPa.mm, the fracture toughness of this material has been measured to be 32 MPa.mm [8]. However, by applying the in-plane and out-of-plane loadings, this value is reduced to about 20 MPa.mm.

The effect of load triaxiality on the fracture mechanism was also investigated. Scanning electron microscopy was conducted on the fracture surface of the specimens. Figure 6 shows examples of the SEM images in two extreme cases. The governing mechanism of fracture in both specimens was void nucleation, and growth coalescence. However, regions of transgranular fracture can be observed in the specimen with high constraint level. It can be argued that since an essential parameter in void nucleation, and growth coalescence mechanism is plastic deformation, high triaxiality that limits the plasticity delays this mechanism. In some areas, then, the energy required to initiate transgranular fracture becomes less than the required energy for void nucleation leading

to the occurring of transgranular fracture. Theoretically, there can be assumed to be a case of pure hydrostatic stress where no plasticity precedes the fracture. Such a condition, where theoretically the triaxiality factor approaches infinity (i.e. zero von-Mises stress), is assumed to be the point that the minimum critical  $J$ -integral is obtained with evidence of transgranular fracture.

## CONCLUSION

- A critical  $J$ -integral much less than the standard fracture toughness values was obtained in specimens under triaxial loading.
- Stress triaxiality factor can be used to relate contributions of both in-plane and out-of-plane constraints.
- Transgranular fracture regions were observed in Aluminium 2024 at room temperature in very highly constrained specimens.

## ACKNOWLEDGEMENT

The financial sponsorship for this work provided by Engineering and Physical Sciences Research Council (EPSRC) of the UK government is gratefully acknowledged. The authors would like to thank Professor Peter Flewitt for his help on interpreting the SEM pictures.

## REFERENCES

1. Sherry, A.H., D.G. Hooton, D.W. Beardsmore, and D.P.G. Lidbury, *Engineering Fracture Mechanics*, 2005. **72**: p. 2396-2415.
2. Sherry, A.H., M.A. Wilkes, D.W. Beardsmore, and D.P.G. Lidbury, *Engineering Fracture Mechanics*, 2005. **72**: p. 2373-2395.
3. ASTM-E399. Annual Book of ASTM standards. Vol. 03.01. 2004: ASTM.
4. Mostafavi, M., D.J. Smith, and M.J. Pavier, *Fatigue and Fracture of Engineering Materials and Structures*, 2010. **Accepted for publication**.
5. Mostafavi, M., M.J. Pavier, and D.J. Smith, in *ESIA10*. 2009: Manchester, UK.
6. ABAQUS. 2006: ABAQUS Inc., Providence, Rhode Island, Version 6.6.
7. Li, F.Z., C.F. Shih, and A. Needleman, *Engineering Fracture Mechanics*, 1985. **21**(2): p. 405-421.
8. Mostafavi, M., D.J. Smith, and M.J. Pavier, *Fatigue and Fracture of Engineering Materials and Structures*, 2008. **32**: p. 5-17.